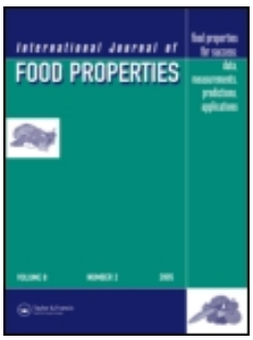

International Journal of Food Properties

ISSN: 1094-2912 (Print) 1532-2386 (Online) Journal homepage: https://www.tandfonline.com/loi/ljfp20

Application of Image Analysis Combined with Computational Expert Approaches for Shrimp Freshness Evaluation

Mahdi Ghasemi-Varnamkhasti, Reza Goli, Michele Forina, Seyed Saeid Mohtasebi, Sahameh Shafiee & Mojtaba Naderi-Boldaji

To cite this article: Mahdi Ghasemi-Varnamkhasti, Reza Goli, Michele Forina, Seyed Saeid Mohtasebi, Sahameh Shafiee & Mojtaba Naderi-Boldaji (2016) Application of Image Analysis Combined with Computational Expert Approaches for Shrimp Freshness Evaluation, International Journal of Food Properties, 19:10, 2202-2222, DOI: 10.1080/10942912.2015.1118386

To link to this article: https://doi.org/10.1080/10942912.2015.1118386

Accepted author version posted online: 17 Nov 2015.
Published online: 16 Jun 2016.

International Journal of Food Properties, 19:2202–2222, 2016

ISSN: 1094-2912 print/1532-2386 online
DOI: 10.1080/10942912.2015.1118386

Taylor & Francis
Taylor & Francis Group

Application of Image Analysis Combined with Computational Expert Approaches for Shrimp Freshness Evaluation

Mahdi Ghasemi-Varnamkhasti[1], Reza Goli[1], Michele Forina[2], Seyed Saeid Mohtasebi[3], Sahameh Shafiee[4], and Mojtaba Naderi-Boldaji[1]

[1]*Department of Mechanical Engineering of Biosystems, Shahrekord University, Shahrekord, Iran*
[2]*Department of Drug and Food Chemistry and Technology, University of Genoa, Genoa, Italy*
[3]*Department of Agricultural Machinery Engineering, University of Tehran, Karaj, Iran*
[4]*Department of Agricultural Machinery Engineering, Tarbiat Modares University, Tehran, Iran*

This study was aimed to evaluate the freshness and quality of cultured shrimp (*litopenaeus vannamei*) during 9 days of storage on ice (i.e., at a temperature of 0°C) using image processing technique. A lighting chamber was used to provide uniform conditions for illumination. The shrimp freshness was evaluated using computer vision technique through color changes of head, legs and tail of the harvested shrimps. Thirty-six color parameters of the images such as mean and variance of red (r), green (g), blue (b), lightness hue (h), saturation (s), value (v), luma information (i and y), the luma component (y), chroma component (cr), lightness (L^*), redness (a^*), yellowness (b^*), chroma (c), and hue (h) were analyzed. Some parameters, such as b^*, from side pictures and r mean, b variance, v mean, y mean, b^* mean and (L^*) mean from top pictures changed with a rather similar trend during the storage period. Different computational expert approaches such as linear discriminant analysis, quadratic discriminant analysis, K nearest neighbors, and discriminant partial least squares regression were examined for shrimp freshness classification. For this, all the variables and the subsets of variables were selected by means of stepwise linear discriminant analysis, stepwise orthogonalization, classification and regression trees. The shrimp freshness was characterized with a high classification accuracy of 90%. Freshness evaluation using image processing is proposed as a potential technique to the food industry.

Keywords: Shrimp, Expert approaches, Image analysis, Color, Regression trees.

INTRODUCTION

Shrimp is one of the most delicious seafood, with a high nutritional value and many health benefits.[1] From different types of shrimp, pacific white shrimp (*litopenaeus vannamei*) makes up about 90% of the shrimp aquaculture in the western hemisphere and its global harvest is on the increase.[2] Increasing production and consumption of shrimp can cause to double the importance of its freshness and quality in shrimp industry. Determination of the quality indicators is one of the

Received 11 July 2015; accepted 6 November 2015.
Address correspondence to Mahdi Ghasemi-Varnamkhasti, Department of Mechanical Engineering of Biosystems, Shahrekord University, Shahrekord 88186 34141, PO Box 115, Iran. E-mail: ghasemymahdi@gmail.com
Color versions of one or more of the figures in the article can be found online at www.tandfonline.com/ljfp.

interesting topics in food engineering and the respective industry. For instance, freshness as a qualitative index, is one of the main parameters for evaluating the food products and their preferences by consumers.[3–5]

Shrimp color change depends on several factors of which the microbiological and chemical processes such as changes in protein, lipid fractions, and system of natural enzymes are of particular importance. Existing enzymes in the air may also cause chemical changes on the surface of the shrimp leading to the formation of brown spots near the shrimp surfaces and shell.[3]

Color change of shrimp usually emerges with spots or melanoses being nutritionally harmless but with unpleasant color appearing mainly along the head, swimmerets, tail, and close to shell areas.[6] Some studies have shown that the quality and freshness of sea foods during storage are strongly related to their color.[2,7] Similarly, color can be an important feature in freshness evaluation of shrimp. Freshness and food quality grading system by image processing is based on visual characteristics such as color, texture, and morphology as pointed out by Nagalakshmi et al.[8] This system offers a low-cost, fast-response, and highly accurate technique for food quality grading.

The shrimp freshness and quality can be determined using a range of destructive and nondestructive methods including the sensory methods (e.g., quality index method [qim], torry scheme, etc.), physical methods (e.g., texture analysis, torrymeter, electronic nose, and near-infrared reflectance spectroscopy), chemical and biochemical methods (e.g., total volatile basic nitrogen, trimethylamine, pH, atp, etc.), and microbiological methods (i.e., the total plate count of bacterial load).[9,10] Sun et al.[11] studied the effect of grape seed extracts (GSE) on the melanosis and quality of pacific white shrimp during storage on ice. Their results suggested that GSE could be used as an efficient natural agent to hinder postmortem melanosis to improve the quality of shrimp during storage.

The quality or freshness evaluation of the aquatic foods has been previously reported.[12,13] However, only a few studies can be found that apply computer vision systems for quality evaluation of shrimp. For instance, Luzuriaga et al.,[14] developed an automated device in red-green-blue (RGB) color space for diagnosing melanosis and detection of foreign objects. Their machine vision system measured the percent area of melanosis on white shrimp (*penaeus setiferus*) stored on ice for up to 17 days. Melanosis was measured and predicted with grading of a trained sensory panel. This approach could objectively characterize the visual quality indices of white shrimp. The aim of this study was to assess the potential of image analysis (color and texture properties) as a reliable method for shrimp freshness evaluation. For this purpose, several computational expert approaches were used.

MATERIALS AND METHODS

Pacific white shrimps, weighing between 10 to 25 g, were purchased from a shrimp farm in Booshehr, Iran. Immediately after harvesting, the shrimps were dipped into sodium sulfites, then transported to the laboratory in polystyrene boxes filled with ice. All shrimps were stored on ice at a temperature of 0–4°C for 9 days. For avoiding the contact between shrimps and the accumulated water, every 10 shrimps were packed into a plastic pocket. Imaging was performed immediately after harvest and every 72 h, i.e., on the 3rd, 6th, and 9th days of storage.

The image processing system consisted of a dark chamber and lighting system, a digital camera, computer hardware, and software. For a proper illumination of the shrimp samples, some light-emitting diode (LED) lamps with white and yellow colors were installed on the upper part of the dark chamber. To prevent the direct incidence of light to the sample and its reflection, polyvinyl chloride (PVC) sheets were used in front of the lamps. The lighting box was made with aluminum. To minimize the background light and light reflectance, the interior walls of the lighting chamber were covered with black sheet. To adjust the distance between the samples and camera, the

chamber was equipped with a knob adjusted by rotary moving. The best quality of image was found at a distance of 11 cm over the sample. A charge-coupled device (CCD) power shot color camera (Sony dsc-w530 digital color camera, Japan,) with remote capturing capability was employed to take images from the shrimp samples. The camera was connected to a laptop (ASUS, k43sa, China) through universal serial bus (USB) port. The shrimp sample was located on the center of the background (Fig. 1a). Images were captured with a five megapixel resolution. For stable lighting, the camera and LED lamps were turned on 10 min before capturing the images. For calibrating the camera, the white balance adjustment was manually applied. All images were taken with the same camera specifications (exposure mode: manual, no zoom, no flash, image type: jpeg). After setting the best illumination, skin images of 80 shrimps on four days (0, 3, 6, and 9 days of storage) were taken by means of the digital camera and the resulting images were transferred to the computer. The required programs for processing the images and extracting the desired features were written using the image processing functions in MATLAB software.[15] Freshness of the shrimp was then characterized based on the four categories of freshness (i.e., four storage days). Characterization was based on texture and color parameters of skin including average color of the head, legs, and the tail.

The image preprocessing steps are presented in Figs. 1b and 1c. Image pre-processing generally includes suppressing the low-frequency background noise, normalizing the intensity of each image particle to correct the geometric distortions, grey level, blurring, and omitting the reflections and image portion masking. After image acquisition and storage, all images were in a "jpeg" format

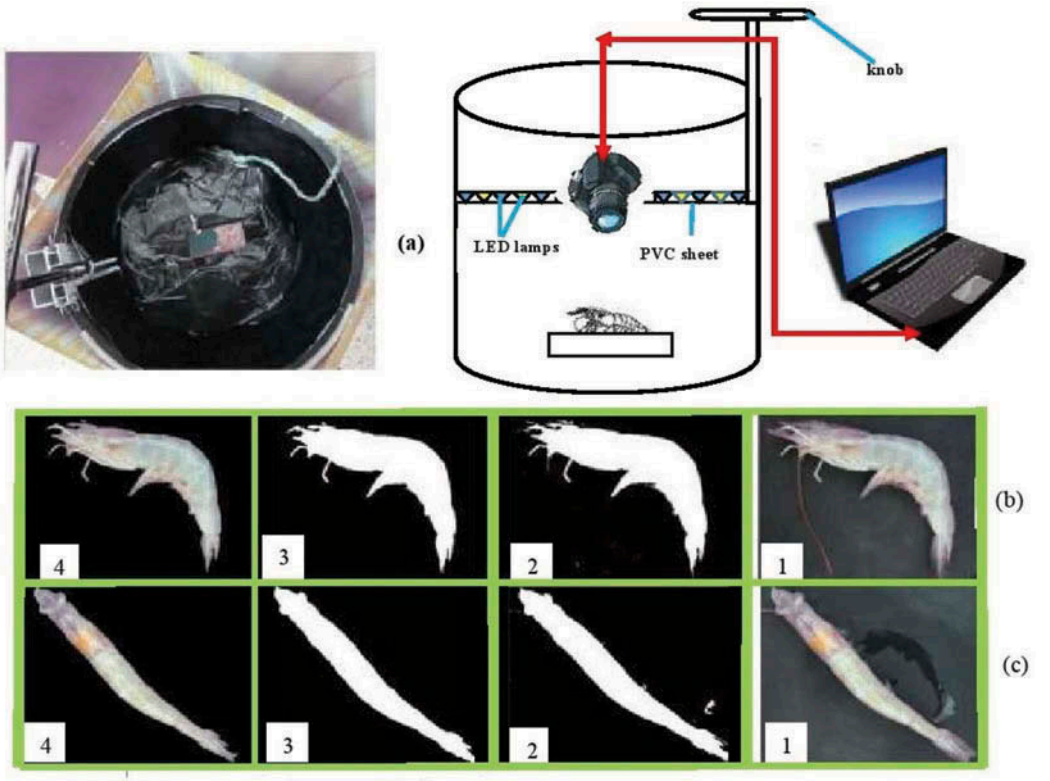

FIGURE 1 A: Lighting chamber for image capturing; B: shrimp side pictures; and C: shrimp top pictures.

with a resolution of 757 × 1050 with RGB color mode. A black background was used for each sample for imaging (Figs. 1b and 1c). All images were converted to binary image and Otsu thresholding method was used for separating the particles from the background.[16,17] Then, the resulting image was subtracted from the original image (Figs. 1b2 and 1c2). Moreover, voids in the resulting image were filled with their neighboring intensities (Figs. 1b3 and 1c3). The features were then extracted from the basic color image combined with the binary image (Figs. 1b4 and 1c4). The data matrix has 80 rows (objects, i.e., 20 shrimp samples for each storage time) and 66 columns (i.e., variables). The variables are defined in Table 1.

Data analysis was performed in MATLAB by means of explorative analysis (principal components analysis) and the following classification techniques:[18] (1) linear discriminant analysis (LDA), (2) quadratic discriminant analysis (QDA), (3) K nearest neighbors (KNN), and (4) discriminant partial least squares regression (D-PLS). The items, both from the variables and the subsets of variables, were selected by means of stepwise-LDA (STEP-LDA), Stepwise orthogonalization (SELECT), and classification and regression trees (CART).[5]

RESULT AND DISCUSSION

Figure 2 shows the changes in color of different parts of shrimp body during storage on ice for 9 days. It is clear that the color of shrimp head, tail, and legs changed sequentially to orange color (3rd day), brown (6th day), and dark (9th day) during the period of storage. This could be attributed to the activity of microorganisms leading to organoleptic changes in color and appearance of shrimp after death.[19] Okpala et al.[20] found that color changes of pacific white shrimp freshly harvested is associated with the development of rancid odors during frozen storage. Also, the metric chroma (c) and total color difference (TCD) could be used to determine freshness and shelf life of pacific white shrimp freshly harvested and stored on ice. Their results were not in agreement with the color data of deep water pink shrimp (*parapenaeus longirostris*) processed on board with ice as found by Huidobro et al.[21]

As illustrated in Fig. 3, on the day 0 (i.e., immediately after harvest) no melanosis, flesh, and spot could be found on shrimp skin. On the third day, a small part of the shrimp head, legs, and tail became slightly dark. Black dots may not be harmful but can be an indication of poor cooling, transportation, and storage of shrimp after harvest. Figure 4a shows that the means of r, g, and b of side pictures decreased during shrimp storage. This observation could be related to increase in melanosis during storage time. The h and s increased until the 6th day and slightly decreased between 6th to 9th days while v continuously decreased over the 9 days as shown in Fig. 4b. The change trends of L^*, a^*, and b^* during storage are depicted in Fig. 4c. It can be seen that L^* decreased over the storage time while a^* and b^* did not show any significant change.

Figure 4d shows the change in chroma (c) and hue (h). The hue rapidly increased until the 6th day followed by a sharp decrease between the 6th to 9th day. However, the chroma remained almost constant. Similar variations were found for the color parameters of top pictures (not shown). A completely randomized block design was used for statistical analysis and Duncans' test was performed for mean comparisons.

General statistics

Table 2 shows some statistical parameters of the variables obtained from the images. For standardization of the variables, autoscaling, i.e., centering and dividing by the standard deviation was applied on the data. The correlation analysis (Fig. 5) showed that the last 20 variables are

TABLE 1
The variables extracted from the images captured

Variable	*Description*
mean_l	means of lightness
mean_a	means of redness
mean_b	means of yellowness
mean_h	means of lightness hue
mean_s	means of saturation
mean_v	means of value
Rcontrast	Red color contrast
Rhomogeneity	Red homogeneity
Renergy	Red energy
RCorrelation	Red Correlation
Rentropy	Red entropy
Gcontrast	Green color contrast
Ghomogeneity	Green homogeneity
Genergy	Green energy
GCorrelation	Green Correlation
Gentropy	Green entropy
Bcontrast	blue color contrast
Bhomogeneity	blue homogeneity
Benergy	blue energy
BCorrelation	blue Correlation
Bentropy	blue entropy
Hcontrast	hue color contrast
Hhomogeneity	hue homogeneity
Henergy	hue energy
HCorrelation	hue Correlation
Hentropy	hue entropy
Scontrast	saturation contrast
Shomogeneity	saturation homogeneity
Senergy	saturation energy
SCorrelation	saturation Correlation
Sentropy	saturation entropy
Vcontrast	value contrast
Vhomogeneity	value homogeneity
Venergy	value energy
VCorrelation	value Correlation
Ventropy	value entropy
glcmRmean	means of Red gray-level co-occurrence matrix (GLCM)
glcmGmean	means of Green gray-level co-occurrence matrix (GLCM)
glcmBmean	means of blue gray-level co-occurrence matrix (GLCM)
glcmHmean	means of hue gray-level co-occurrence matrix (GLCM)
glcmSmean	means of saturation gray-level co-occurrence matrix (GLCM)
glcmVmean	means of value gray-level co-occurrence matrix (GLCM)

highly correlated (i.e., with correlation coefficients > 0.98). The Fisher Weights (FW)[22] for the variable v and the categories 1 and 2 were calculated by:

$$FW_v = \frac{\left(\bar{x}_{v1} - \bar{x}_{v2}\right)^2}{\sum_{i=1}^{I_1} \frac{\left(x_{iv1} - \bar{x}_{v1}\right)^2}{I_1} + \sum_{i=1}^{I_2} \frac{\left(x_{iv2} - \bar{x}_{v2}\right)^2}{I_2}} \quad (1)$$

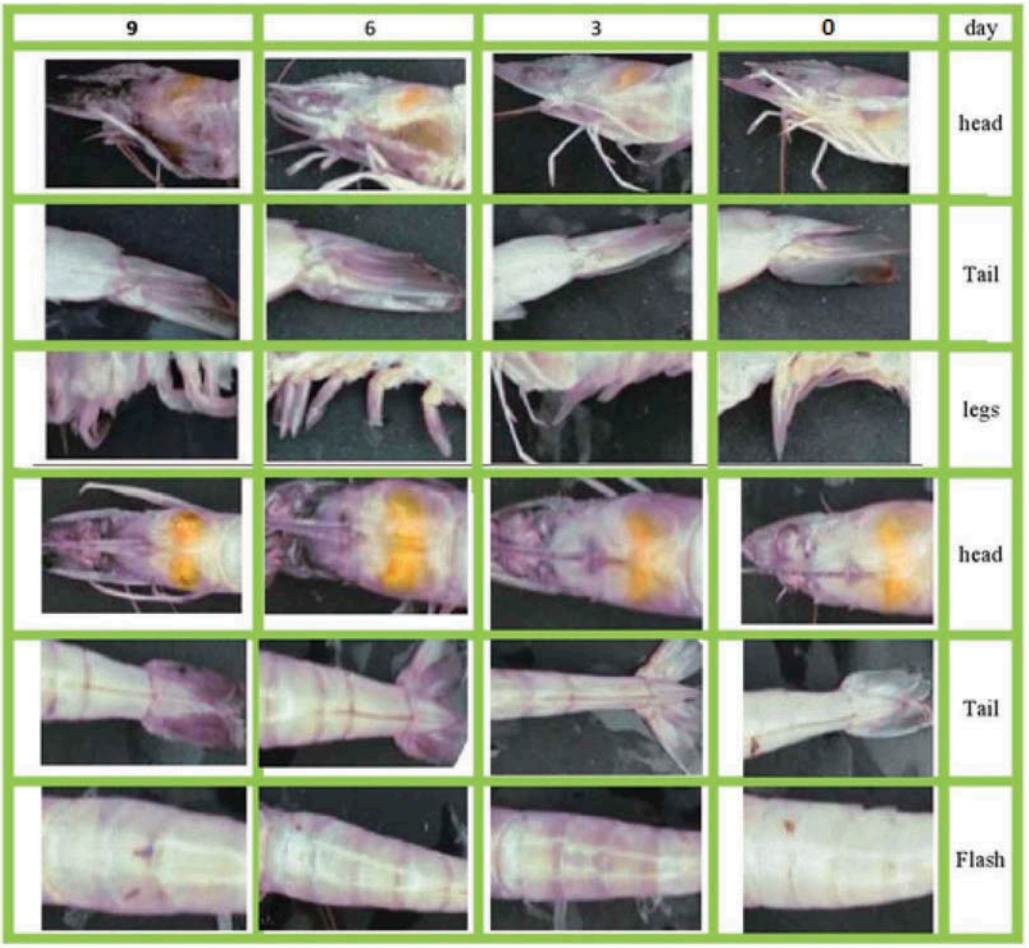

FIGURE 2 Cultured shrimp color changes during storage on ice.

Or

$$FW_v = 2\,\frac{(\bar{x}_{v1} - \bar{x}_{v2})^2/4}{\dfrac{\sum_{i=1}^{I_1}\frac{(x_{iv1}-\bar{x}_{v1})^2}{I_1} + \sum_{i=1}^{I_2}\frac{(x_{iv2}-\bar{x}_{v2})^2}{I_2}}{2}} \tag{2}$$

where I_1 and I_2 are the numbers of objects (i.e., samples) in the two categories, X_{iv1} is the value of the variable v for object I in category 1 and X_{v1} is the mean of variable 1 in category 1. In Eq. (1), the numerator is the between-centroids variance of the samples. Note that the diminution of the degrees of freedom is not considered. The denominator is the mean of the two within-category variances. In a case where the categories are more than 2, the FW are the mean of the weights for all pairs of the categories. FW > 10 indicates an excellent separation of the categories and FW > 1 indicates a significant separation. FW in Tables 3a–g show that some variables have a good discriminant power, especially for some pairs of categories. Table 4 presents the FW of some variables and sums of the standardized (not centered) variables. For each class, the most

FIGURE 3 The color change of four groups of pacific white shrimps (*litopenaeus vannamei*) during 9 days of storage on ice.

discriminant variables and sums were selected. Then, the four selections were joined with the elimination of the duplicated variables.

Principal component analysis (PCA)

PCA applies an orthogonal rotation in the space of the variables. The result is a new set of variables, the principal components, and the linear combinations of the original variables by means of the cosines of the rotation angles. The principal components are not correlated; therefore, each component shows independent information. Moreover, they are ordered according to their variances and generally only few components retain significant information. In the case of PCA (Table 5, Fig. 6) with all the variables, the variance of the first component was found to be 34% of the total variance and that of the second component was 18.1% as compared with 1.5% found for the original variables.

PCA shows a large overlap of the four categories. However, the first component is correlated with the order of the categories, from right for category 1 to left for category 4. The second component shows the presence of two "outliers" (objects 67 and 68 from class 4). PCA was also applied to the 14 variables autoscaled. The separation among the four classes was found to be better, especially for the first class (Fig. 7). It can be stated that object 57 (17 of class 3, green) is responsible for the overlap of class 3 with class 1 (red).

Classification Analysis

The computational approaches for the classification of the freshness categories are given and discussed as follows.

LDA

LDA was applied to the first 20 principal components of the autoscaled data that retain more than 98% of the variance. For each cancellation group, the LDA models were computed. The "canceled" objects (one-fifth) were used for prediction and others (the training set) were considered

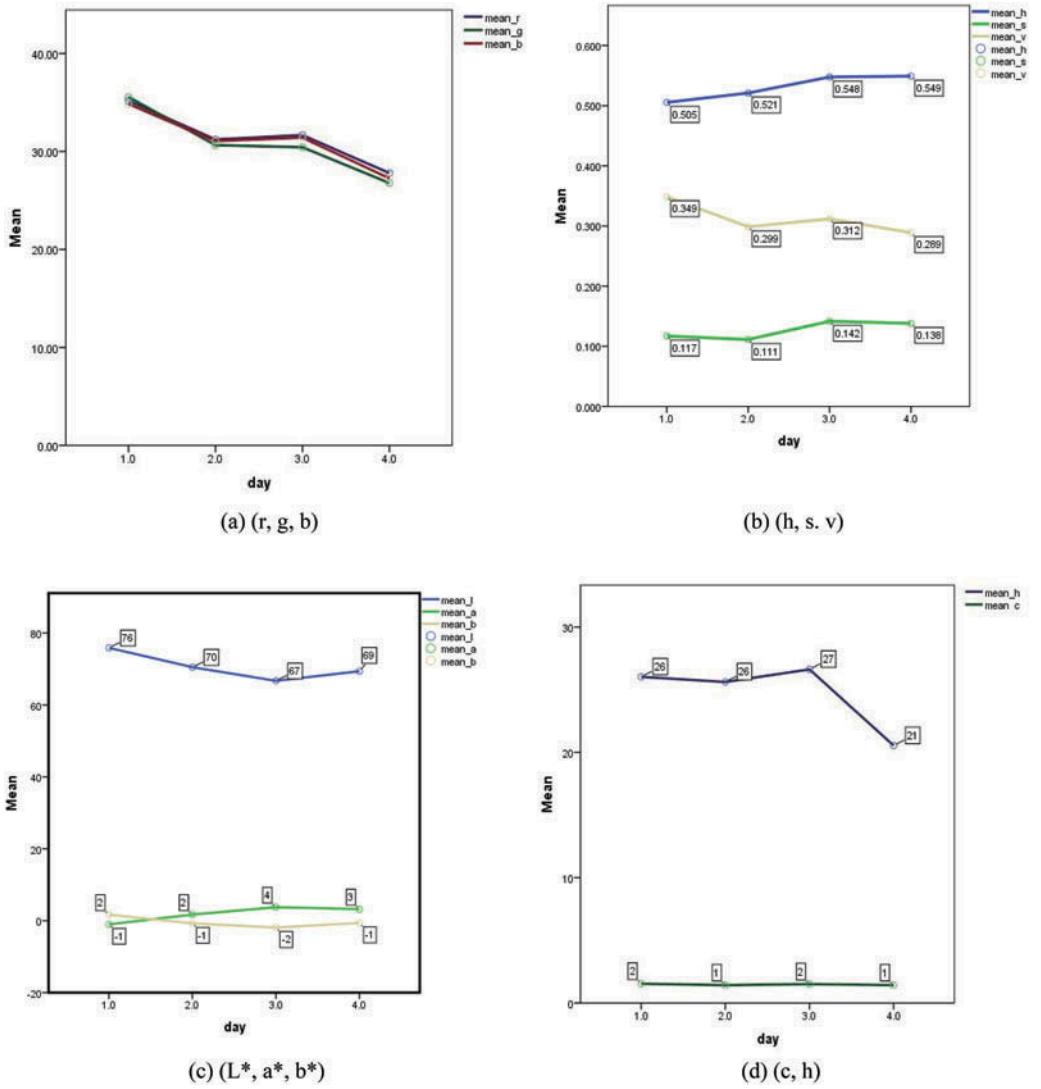

FIGURE 4 Variation of shrimp color parameters from side pictures during storage on ice; A: r, g, and b; B: h, s, and v; C: L^*, a^*, and b^*; and D: c and h.Day: 1 = first day, 2 = third day, 3 = sixth day, 4 = ninth day; h = hue, c = chroma.

to compute the models for classification so that each object was predicted one time and classified four times. The final model was obtained with all the objects in the training set. Results indicated an excellent classification and a relatively good prediction rate. Figure 8 shows the results of the final model. In part A of Fig. 8, the difference between the scores of the objects for class 1 and those for class 3 versus the difference between class 1 and 2 separates perfectly the four classes. We also computed a prediction loss where the errors are weighed according to the distance between the real and the predicted categories, i.e., a measure of the difference between reference and predicted

TABLE 2
Statistics of the variables

Variable no.	*Name of variable*	*Mean*	*Std*	*Asymmetry*	*Minimum*	*Maximum*	*Range*
49	glcmRrange	704797	143686	1.1603	296717	1418603	1121886
52	glcmGrange	629731	178345	1.3374	360667	1404951	1044284
58	glcmHrange	593060	158837	1.8553	347863	1326154	978291
64	glcmVrange	605333	176884	1.4446	351729	1317575	965846
55	glcmBrange	607804	174330	1.4575	359247	1320592	961345
61	glcmSrange	603266	120685	2.2910	439472	1199375	759903
51	glcmRvar	43494	7248	2.9193	35727	80564	44837
66	glcmVvar	43006	7423	3.0559	36275	80878	44604
57	glcmBvar	42982	7432	3.0706	36368	80851	44483
54	glcmGvar	43038	7529	3.0425	36009	80325	44316
60	glcmHvar	43709	7518	3.0834	37400	81523	44123
63	glcmSvar	43702	7097	3.0399	37881	79049	41168
50	glcmRmean	16345	2734	3.1304	14198	29981	15784
53	glcmGmean	16345	2734	3.1304	14198	29981	15784
56	glcmBmean	16345	2734	3.1304	14198	29981	15784
59	glcmHmean	16345	2734	3.1304	14198	29981	15784
62	glcmSmean	16345	2734	3.1304	14198	29981	15784
65	glcmVmean	16345	2734	3.1304	14198	29981	15784
4	l_var	4422	802	0.4824	2988	6771	3783
9	b_range	52.91	12.34	0.1697	23.00	82.00	59.00
7	l_range	235.6	8.3	0.1011	219.0	255.0	36.0
1	mean_l	32.27	5.82	0.5965	19.98	53.02	33.04
8	a_range	33.43	2.11	0.4930	28.00	40.00	12.00
3	mean_b	127.9	0.4	0.2737	127.1	129.2	2.1
6	b_var	127.9	0.4	0.2737	127.1	129.2	2.1
2	mean_a	128.3	0.4	0.0035	127.4	129.2	1.8
5	a_var	128.3	0.4	0.0035	127.4	129.2	1.8
16	h_range	0.7121	0.1866	-0.4920	0.3157	0.9302	0.6146
17	s_range	0.6347	0.1339	-0.0895	0.3251	0.9000	0.5749
38	Hentropy	0.1270	0.1231	0.5932	0.0000	0.4489	0.4489
18	v_range	0.6642	0.1049	-0.6649	0.4039	0.8471	0.4431
21	Renergy	0.4840	0.0831	-0.7829	0.2141	0.6387	0.4245
26	Genergy	0.4133	0.0959	0.2830	0.2555	0.6319	0.3764
43	Sentropy	0.948	0.064	-2.5883	0.625	1.000	0.375
46	Venergy	0.3953	0.0969	0.5437	0.2653	0.6351	0.3698
31	Benergy	0.3960	0.0941	0.4959	0.2654	0.6222	0.3568
36	Henergy	0.3979	0.0631	0.4650	0.2810	0.5524	0.2714
34	Hcontrast	0.3004	0.0610	0.3345	0.1764	0.4474	0.2710
12	mean_v	0.3113	0.0345	0.4643	0.2232	0.4274	0.2042
41	Senergy	0.4747	0.0455	1.0477	0.4126	0.5932	0.1806
10	mean_h	0.5243	0.0287	0.4050	0.4823	0.5810	0.0987
37	HCorrelation	0.9001	0.0176	-0.2222	0.8550	0.9377	0.0827
19	Rcontrast	0.0547	0.0154	1.1051	0.0286	0.1101	0.0815
24	Gcontrast	0.0638	0.0194	0.2229	0.0291	0.1050	0.0759
11	mean_s	0.1247	0.0183	-0.0882	0.0923	0.1619	0.0696
44	Vcontrast	0.0643	0.0181	0.0513	0.0310	0.0996	0.0687
29	Bcontrast	0.0647	0.0172	0.0399	0.0316	0.0966	0.0651
42	SCorrelation	0.9150	0.0134	-0.3285	0.8824	0.9428	0.0604
23	Rentropy	0.992	0.010	-1.8335	0.954	1.000	0.046
20	Rhomogeneity	0.9729	0.0077	-1.1184	0.9450	0.9858	0.0407
25	Ghomogeneity	0.9683	0.0096	-0.2190	0.9481	0.9855	0.0373

(*continued*)

TABLE 2
(*Continued*)

Variable no.	*Name of variable*	*Mean*	*Std*	*Asymmetry*	*Minimum*	*Maximum*	*Range*
39	Scontrast	0.0489	0.0091	0.7569	0.0334	0.0706	0.0372
28	Gentropy	0.994	0.007	-1.7581	0.965	1.000	0.035
33	Bentropy	0.994	0.007	-1.6124	0.965	1.000	0.035
48	Ventropy	0.994	0.007	-1.7600	0.965	1.000	0.035
45	Vhomogeneity	0.9681	0.0089	-0.0425	0.9509	0.9845	0.0337
30	Bhomogeneity	0.9679	0.0085	-0.0338	0.9524	0.9842	0.0318
27	GCorrelation	0.9863	0.0047	-1.4909	0.9690	0.9923	0.0233
15	v_var	0.0352	0.0048	0.0964	0.0253	0.0479	0.0226
32	BCorrelation	0.9859	0.0046	-1.2468	0.9710	0.9923	0.0213
13	h_var	0.0227	0.0042	0.7387	0.0155	0.0345	0.0190
40	Shomogeneity	0.9757	0.0045	-0.7191	0.9650	0.9837	0.0187
47	VCorrelation	0.9876	0.0039	-1.1195	0.9758	0.9932	0.0173
35	Hhomogeneity	0.9729	0.0036	0.2514	0.9655	0.9815	0.0160
22	RCorrelation	0.9892	0.0031	-0.9453	0.9795	0.9948	0.0153
14	s_var	0.0026	0.0007	0.3683	0.0015	0.0044	0.0029

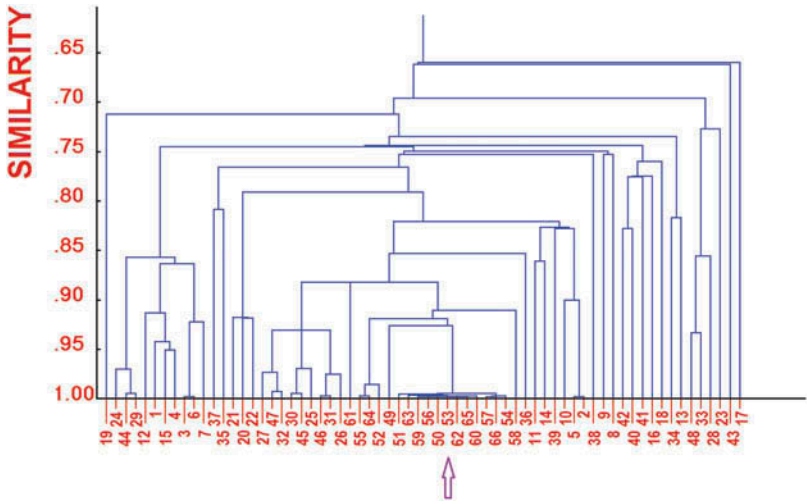

FIGURE 5 Correlation tree among the variables, shown as dendrogram of the similarities (correlation coefficients) obtained by means of the single linkage method. The arrow indicates the group of much correlated variables.

freshness. For instance, when a sample of class 3 is predicted in class 4, the error has weight 1; when it is predicted in class 1 the error has weight 2. Prediction loss for LDA was found

KNN

KNN classifies each object according to the class of its KNN. The method was used with K = 1, 3, 5. The best results were obtained with K = 1 (1NN). In each of the five cancellation groups of cross validation, the non-canceled objects (here 64 objects) are predicted using the distances from

TABLE 3A
General fisher weights

Order	*Variable*	*FW*	*Index of variable*
1	mean_s	1.81768	11
2	mean_a	1.80385	2
3	a_var	1.80385	5
4	mean_h	1.39050	10
5	s_var	1.34800	14
6	mean_v	1.16282	12
7	glcmHrange	1.03916	58
8	glcmGrange	0.93738	52
9	HCorrelation	0.81493	37
10	Genergy	0.79556	26
11	glcmBrange	0.77957	55
12	Senergy	0.76862	41
13	glcmVrange	0.76339	64
14	l_var	0.75940	4
15	mean_b	0.75889	3
16	b_var	0.75889	6
17	Shomogeneity	0.73622	40
18	Scontrast	0.72532	39
19	Venergy	0.71213	46
20	Benergy	0.71163	31
21	Hhomogeneity	0.71087	35
22	a_range	0.68911	8
23	Gcontrast	0.65230	24
24	Ghomogeneity	0.64979	25
25	l_range	0.59323	7
26	Henergy	0.56208	36
27	mean_l	0.55357	1
28	glcmGvar	0.53779	54
29	glcmRrange	0.53547	49
30	glcmRvar	0.53230	51

all the other non-canceled objects (here 63 objects). In the final run, without canceled objects, each object is classified using the distance from all the remaining objects (here 79 objects). Then, each object is classified one time and predicted four times. The classification ability (Table 6) of 1NN was found to be poorer than that of LDA, but the prediction ability is better (although not significantly different). Prediction loss for KNN was found to be 14.2 (KNN predicts five times, so that from the prediction matrix, the loss is computed as 71.5).

QDA

QDA needs a larger ratio of the number of objects to variables compared with LDA. Hence, it was applied to the first 15 principal components of the autoscaled data which retain about 96% of the variance. The classification ability was found to be 97.5%. This result can be explained by the fact that the space of class 1 is relatively small in comparison with the other classes. Figure 9 shows the QDA class spaces. The ellipses correspond to the same Mahalanobis distance from the class centroids so that almost all the objects are accepted from the model of class 4 and many

TABLE 3B
Fisher weights for categories 1 and 2

Order	*Variable*	*FW*	*Index of variable*
1	mean_v	2.59850	12
2	mean_a	1.93064	2
3	a_var	1.93064	5
4	l_range	1.75111	7
5	Benergy	1.30074	31
6	Venergy	1.27149	46
7	l_var	1.25436	4
8	mean_b	1.23805	3
9	b_var	1.23805	6
10	Genergy	1.19190	26
11	glcmGrange	1.18379	52
12	glcmBrange	1.16927	55
13	glcmVrange	1.12184	64
14	Vhomogeneity	1.02947	45
15	Vcontrast	1.01744	44
16	Bhomogeneity	0.95099	30
17	Bcontrast	0.93443	29
18	Ghomogeneity	0.87467	25
19	Gcontrast	0.86510	24
20	Hcontrast	0.83693	34

TABLE 3C
Fisher weights for categories 1 and 3

Order	*Variable*	*FW*	*Index of variable*
1	mean_h	4.78273	10
2	mean_a	4.41163	2
3	a_var	4.41163	5
4	s_var	2.96057	14
5	mean_s	2.34845	11
6	a_range	1.86517	8
7	mean_b	1.86026	3
8	b_var	1.86026	6
9	b_range	1.67028	9
10	Benergy	1.48839	31
11	Genergy	1.43653	26
12	Venergy	1.42884	46
13	l_var	1.42454	4
14	glcmGrange	1.14411	52
15	l_range	1.09884	7
16	glcmBrange	1.06012	55
17	glcmVrange	1.02242	64
18	Ghomogeneity	1.01079	25
19	Gcontrast	0.99278	24
20	mean_v	0.98523	12

TABLE 3D
Fisher weights for categories 1 and 4

Order	*Variable*	*FW*	*Index of variable*
1	mean_a	3.69438	2
2	a_var	3.69438	5
3	s_var	3.00501	14
4	mean_v	2.97945	12
5	glcmGrange	2.21970	52
6	Genergy	2.04087	26
7	Gcontrast	1.93656	24
8	mean_s	1.93081	11
9	Ghomogeneity	1.90340	25
10	mean_h	1.84934	10
11	glcmBrange	1.74047	55
12	glcmVrange	1.72916	64
13	l_var	1.72656	4
14	Shomogeneity	1.72620	40
15	mean_l	1.72268	1
16	Scontrast	1.69613	39
17	Venergy	1.45227	46
18	Benergy	1.37783	31
19	Senergy	1.26653	41
20	glcmGvar	1.24111	54

TABLE 3E
Fisher weights for categories 2 and 3

Order	*Variable*	*FW*	*Index of variable*
1	mean_s	3.48230	11
2	glcmHrange	1.37913	58
3	a_range	1.02949	8
4	Senergy	0.99950	41
5	mean_h	0.97335	10
6	h_range	0.92599	16
7	s_var	0.91014	14
8	Henergy	0.73503	36
9	b_range	0.63133	9
10	mean_a	0.50438	2
11	a_var	0.50438	5
12	Shomogeneity	0.50384	40
13	Scontrast	0.50109	39
14	Renergy	0.45628	21
15	RCorrelation	0.43315	22
16	glcmSrange	0.33341	61
17	Rhomogeneity	0.22344	20
18	Rcontrast	0.22223	19
19	glcmRrange	0.21576	49
20	Ventropy	0.18419	48

TABLE 3F
Fisher weights for categories 2 and 4

Order	*Variable*	*FW*	*Index of variable*
1	mean_s	3.04445	11
2	glcmHrange	2.22633	58
3	HCorrelation	1.81717	37
4	Henergy	1.57999	36
5	h_range	1.40807	16
6	Senergy	1.39403	41
7	Hhomogeneity	1.36529	35
8	Shomogeneity	1.33794	40
9	Scontrast	1.31480	39
10	s_var	1.01352	14
11	glcmHvar	0.91585	60
12	glcmRvar	0.88849	51
13	glcmGvar	0.88571	54
14	glcmRmean	0.86399	50
15	glcmGmean	0.86399	53
16	glcmBmean	0.86399	56
17	glcmHmean	0.86399	59
18	glcmSmean	0.86399	62
19	glcmVmean	0.86399	65
20	glcmBvar	0.84295	57

TABLE 3G
Fisher weights for categories 3 and 4

Order	*Variable*	*FW*	*Index of variable*
1	Hhomogeneity	1.77240	35
2	HCorrelation	1.55413	37
3	a_range	1.13129	8
4	v_range	1.04548	18
5	glcmRvar	1.01147	51
6	glcmHvar	0.98419	60
7	glcmRrange	0.96354	49
8	glcmSvar	0.91367	63
9	glcmRmean	0.91199	50
10	glcmGmean	0.91199	53
11	glcmBmean	0.91199	56
12	glcmHmean	0.91199	59
13	glcmSmean	0.91199	62
14	glcmVmean	0.91199	65
15	glcmGvar	0.90864	54
16	glcmVvar	0.88552	66
17	glcmBvar	0.88193	57
18	glcmHrange	0.74522	58
19	glcmGrange	0.61882	52
20	Hcontrast	0.57892	34

TABLE 4
Fisher weights of a single category (mean of three FW between pairs of categories), for some variables and the most discriminant sums of standardized variables

Variable or sum	*Indexes*	*For class 1*	*For class 2*	*For class 3*	*For class 4*
a_range	8			1.34	
a_var	5	3.35	0.86	1.68	1.33
a_var+b_range	5 + 9	3.65			
a_var+mean_s	5 + 11	4.34		3.30	
a_var+s_var	5 + 14	5.10			
glcmHrange	49	1.52	1.34		1.40
Henergy	36		0.96		
mean_a+glcmGrange	2 + 49				
mean_h	10	2.27		1.92	
mean_s	11		2.18	1.97	1.69
mean_v	12	2.19	0.92		
s_var	14	2.05		1.29	1.34
s_var+Hhomogeneity	14 + 35				3.02
v_range+Shomogeneity	18 40				

TABLE 5
Characteristics of the principal components. Pretreatment: column autoscaling

Component	*Eigenvalue*	*% Expl. variance*	*% Cumulative*
1	22.164490	34.00766	34.008
2	11.814124	18.12677	52.134
3	6.688553	10.26245	62.397
4	4.160877	6.38416	68.781
5	3.437949	5.27495	74.056
6	2.993565	4.59312	78.649
7	2.422498	3.71691	82.366
8	2.101696	3.2247	85.591
9	1.982746	3.04219	88.633
10	1.144770	1.75646	90.389
11	0.988500	1.51669	91.906
12	0.799062	1.22603	93.132
13	0.622273	0.95477	94.087
14	0.582932	0.89441	94.981
15	0.486600	0.74661	95.728
16	0.436219	0.6693	96.397
17	0.364710	0.55959	96.957
18	0.316729	0.48597	97.443
19	0.299984	0.46027	97.903
20	0.211433	0.32441	98.227

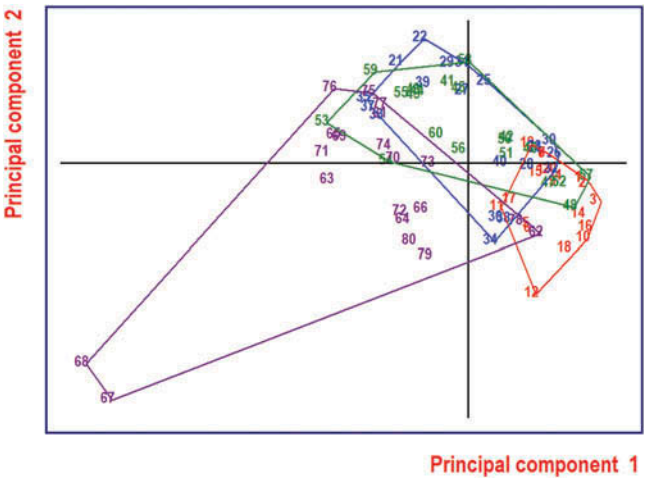

FIGURE.6 Score plot on the two first principal components of all 66 variables (autoscaled). Red: Class1, Blue: Class 2, Green: Class 3, Magenta: Class 4. The convex hulls indicate the dispersion of the classes.

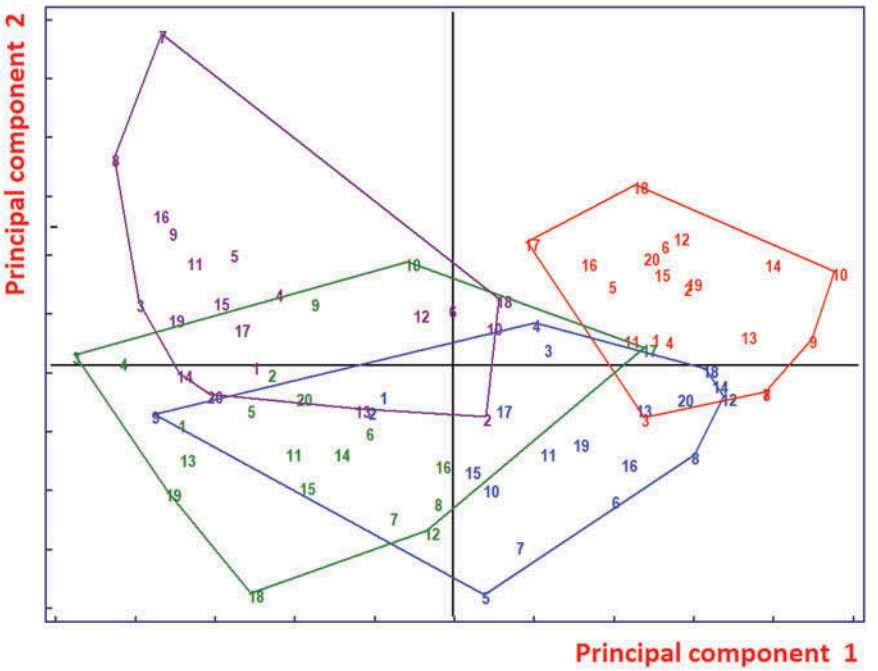

FIGURE 7 Score plot on the two first principal components of the 14 variables/features (autoscaled). Red: class 1, Blue: class 2, Green: class 3, Magenta: class 4.

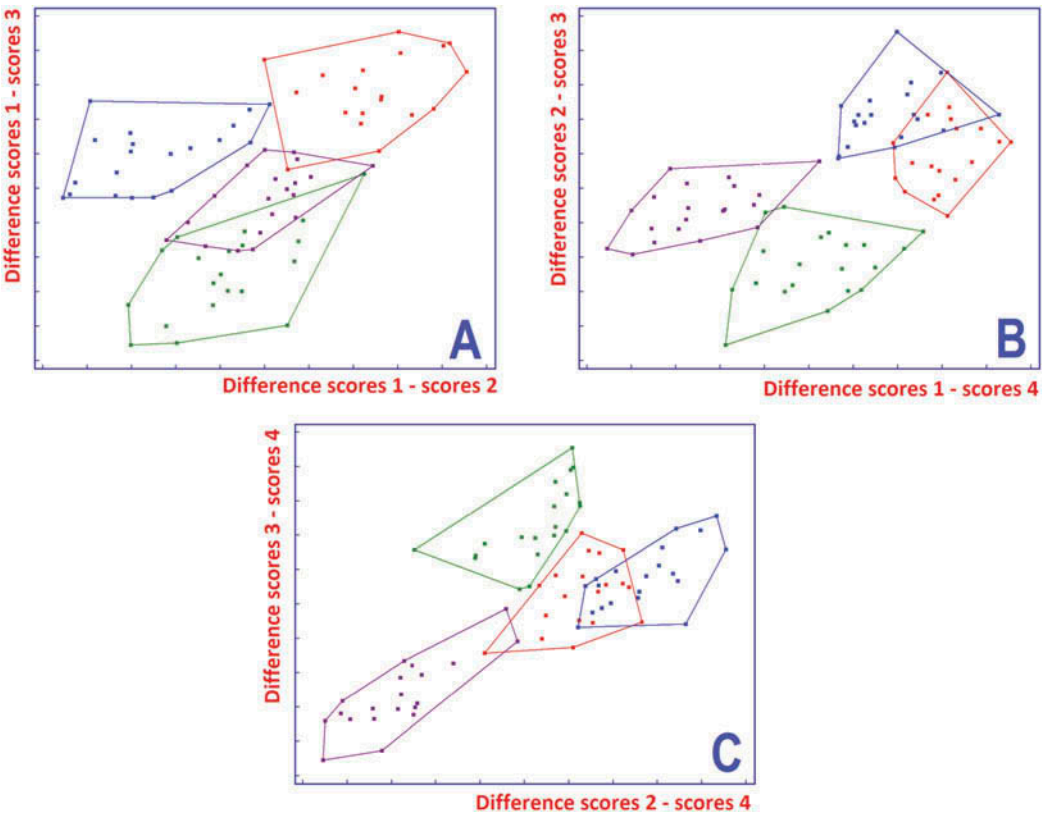

FIGURE 8 Plots of the differences between scores of LDA. Red: class 1, Blue: class 2, Green: class 3, Magenta: class 4.

objects are closest (Mahalanobis distance) to the centroid of class 4 than to the centroid of their true class in spite of a larger Euclidean distance.

Discriminant partial least squares (D-PLS)

The best results were achieved by D-PLS analysis with eight to nine latent variables (Table 7). The smallest prediction loss (i.e., 12) was found by D-PLS analysis.

Results with the selections of variables

Several subsets of variables and linear transforms were checked. The best results were obtained with a combination of classification trees and LDA. Classification trees are hierarchical sequence of splitting the data set by means of binary decisions based on the values of quantitative or ordinal variables. Each decision splits the data set in two subsets. The classification trees are based on a series of splitting of the object, based on the "best" variable.[23,24] The linear combinations used here are LDA discriminant variables. For each combination of two categories and two variables, the LDA canonical variable was computed. For each pair of categories, the canonical variables (their number is selected by the operator) with the largest FW were selected. The result of this procedure was a set of one variable and three transforms:

TABLE 6
Classification and prediction rates of KNN (K = 1), applied to all the autoscaled variables

Classification matrix				
Order	*Assigned to class 1*	*Assigned to class 2*	*Assigned to class 3*	*Assigned to class 4*
Objects of class 1	19	1	0	0
Objects of class 2	2	17	1	0
Objects of class 3	1	0	18	1
Objects of class 4	1	1	1	17
	In class 1	In class 1	In class 1	In class 4
% correct classifications	95.00	85.00	90.00	85.00
% TOTAL	88.75			
Prediction matrix				
Order	Assigned to class 1	Assigned to class 2	Assigned to class 3	Assigned to class 4
Objects of class 1	74	5	1	0
Objects of class 2	12	63	4	1
Objects of class 3	4	0	66	10
Objects of class 4	4	4	8	64
	In class 1	In class 1	In class 1	In class 4
% correct predictions	92.50	78.75	82.50	80.00
% TOTAL	83.44			

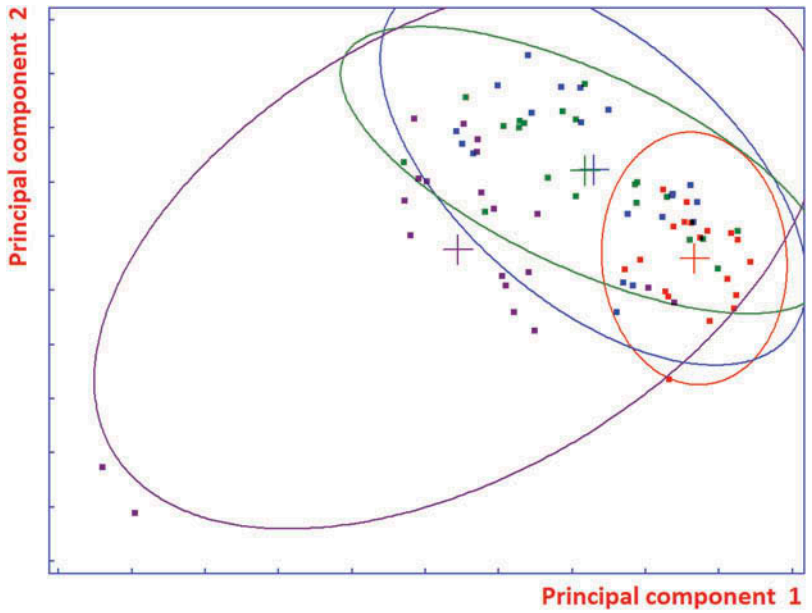

FIGURE 9 95% confidence ellipses computed with T^2 statistics in the space of the two first components.

TABLE 7
Classification and prediction rates of D-PLS (eight latent variables), applied to all the autoscaled variables

Classification matrix				
Order	*Assigned to class 1*	*Assigned to class 2*	*Assigned to class 3*	*Assigned to class 4*
Objects of class 1	20	0	0	0
Objects of class 2	2	18	0	0
Objects of class 3	1	0	19	0
Objects of class 4	0	1	0	19
	In class 1	In class 1	In class 1	In class 4
% correct classifications	100.00	90.00	95.00	95.00
% TOTAL	95.00			
Prediction matrix				
Order	Assigned to class 1	Assigned to class 2	Assigned to class 3	Assigned to class 4
Objects of class 1	18	2	0	0
Objects of class 2	2	17	0	0
Objects of class 3	1	1	17	1
Objects of class 4	0	2	1	17
	In class 1	In class 1	In class 1	In class 4
% correct predictions	90.00	85.00	85.00	85.00
% TOTAL	86.25			

TABLE 8
Classification and prediction rates of LDA applied to the four features selected by means of multivariate classification trees

Classification matrix				
Order	*Assigned to class 1*	*Assigned to class 2*	*Assigned to class 3*	*Assigned to class 4*
Objects of class 1	100	0	0	0
Objects of class 2	10	85	5	0
Objects of class 3	5	0	95	082
Objects of class 4	0	5	13	
	In class 1	In class 1	In class 1	In class 4
% correct classifications	100.00	85.00	95.00	82.00
% TOTAL	90.50			
Prediction matrix				
Order	Assigned to class 1	Assigned to class 2	Assigned to class 3	Assigned to class 4
Objects of class 1	20	0	0	0
Objects of class 2	2	17	1	0
Objects of class 3	1	0	19	0
Objects of class 4	0	1	3	16
	In class 1	In class 1	In class 1	In class 4
% correct predictions	100.00	85.00	95.00	80.00
% TOTAL	90.00			

mean_a + 0.025b_range
glcmHrange
0.00139a_range − Hhomogeneity
0.32mean_v − 0.95h_var

The performance of the LDA model with these four features is shown in Table 8. Prediction loss for LDA decreased to 10. Hence, this is a better result both for the overall prediction ability (90%, eight errors) and for the prediction loss.

As a recommendation, the results of the current study can be coupled with innovative instruments such as electronic noses to monitor the odor of the shrimps during storage.[25,26] During storage, the organoleptic properties of the shrimp samples change. Therefore, odor of the stored shrimp can be gathered and injected into the sensor chamber of an electronic nose to recognize the changes accurately.

CONCLUSIONS

In this study, the potential of classification and prediction of shrimp freshness by image processing and a range of computational expert approaches was evaluated. The images captured from different parts of shrimp body were analyzed immediately after harvest and after 3, 6, and 9 days storage on ice (at a temperature of 0–4°C). The results showed high classification accuracies to recognize the freshness classes from the image parameters. In data analysis, many subsets of variables and linear transforms were checked. The best result was achieved with a combination of classification trees and LDA. Results indicated an excellent classification accuracy around 90% and a relatively good prediction rate. The computer vision system can be used for automated and online evaluation of shrimp quality and freshness. Future research could be aimed for development of a practical instrument for online monitoring and controlling shrimp storage by the use of smart phone cameras.

ACKNOWLEDGMENTS

The authors would like to thank the support of Shahrekord University in this research.

REFERENCES

1. Mohebbi, M.; Akbarzadeh, T.M.-R.; Shahidi, F.; Moussavi, M.; Ghoddusi, H.-B. Computer Vision Systems (CVS) for Moisture Content Estimation in Dehydrated Shrimp. Computers and Electronics in Agriculture **2009**, *69*(2), 128–134.
2. Nollet, L.M.; Toldrá, F. *Handbook of Seafood and Seafood Products Analysis*; CRC Press: Boca Raton, New York, 2010.
3. Rehbein, H.; Oehlenschlager, J. *Fishery Products: Quality, Safety, and Authenticity*; John Wiley & Sons: London, UK, 2009.
4. Ghasemi-Varnamkhasti, M.; Mohtasebi, M.M.; Rodriguez-Mendez, M.L.; Gomes A. A.; Araújo, M.C.U.; Galvão, R. K.H. Screening Analysis of Beer Ageing Using Near Infrared Spectroscopy and the Successive Projections Algorithm for Variable Selection. Talanta **2012**, *89*, 286–291.
5. Ghasemi-Varnamkhasti, M.; Forina, M.; NIR Spectroscopy Coupled with Multivariate Computational Tools for Qualitative Characterization of the Aging Of Beer. Computers and Electronics in Agriculture **2014**, *100*, 34–40.
6. Luzuriaga, D.; Balaban, M. Evaluation of the Odor of Decomposition in Raw and Cooked Shrimp: Correlation of Electronic Nose Readings, Odor Sensory Evaluation, and Ammonia Levels. In *Electronic Noses and Sensor Array Based Systems Design and Applications*; Technomic: Lancaster, PA, USA, 1999.
7. Dowlati, M.; de la Guardia, M.; Dowlati, M.; Mohtasebi, S.S. Application of Machine-Vision Techniques to Fish-Quality Assessment. TrAC Trends in Analytical Chemistry **2012**, *40*, 168–179.

8. Nagalakshmi, S.A.; Mitra, P.; Meda, V.; Color, Mechanical, and Microstructural Properties of Vacuum Assisted Microwave Dried Saskatoon Berries. International Journal of Food Properties **2014**, *17*(10), 2142–2156.
9. Nirmal, N.P.; Benjakul, S. Effect of Catechin and Ferulic Acid on Melanosis and Quality of Pacific White Shrimp Subjected to Prior Freeze–Thawing During Refrigerated Storage. Food Control **2010**, *21*(9), 1263–1271.
10. Shafiee, S.; Minaei, S.; Moghaddam-Charkari, N.; Barzegar, M. Honey Characterization Using Computer Vision System and Artificial Neural Networks. Food Chemistry **2014**, *159*, 143–150.
11. Sun, H.; Lv, H.; Yuan, G.; Fang, X. Effect of Grape Seed Extracts on the Melanosis and Quality of Pacific White Shrimp (*Litopenaeus vannamei*) During Iced Storage. Food Science and Technology Research **2014**, *20*(3), 671–677.
12. Zhang, D.; Lillywhite, K.D.; Lee, D.-J.; Tippetts, B.J. Automatic Shrimp Shape Grading Using Evolution Constructed Features. Computers and Electronics in Agriculture **2014**, *100*, 116–122.
13. Poonnoy, P.; Yodkeaw, P.; Sriwai, A.; Umongkol, P.; Intamoon, S. Classification of Boiled Shrimp's Shape Using Image Analysis and Artificial Neural Network Model. Journal of Food Process Engineering **2014**, *37*, 257–263.
14. Luzuriaga, D.A.; Balaban, M.O.; Yeralan, S. Analysis of Visual Quality Attributes of White Shrimp by Machine Vision. Journal of Food Science **1997**, *62*(1), 113–118.
15. Du, C.; Sun, D. Comparison of Three Methods for Classification of Pizza Topping Using Different Colour Space Transformations. Journal of Food Engineering **2005**, *68*, 277–287.
16. Brosnan, T.; Sun, D.W. Improving Quality Inspection of Food Products by Computer Vision—A Review. Journal of Food Engineering **2004**, *61*(1), 3–16.
17. Gonzalez, R.C.; Woods, R.E.; Eddins, S. Morphological Image Processing. Digital Image Processing **2008**, *3*, 627–688.
18. Tauler, R.; Walczak, B.; Brown, S. *Comprehensive Chemometrics*; Elsevier: Amsterdam, the Netherlands, 2009.
19. Masniyom, P.; Benjama, O.; Maneesri, J. Extending the Shelf-Life of Refrigerated Green Mussel (*Perna Viridis*) Under Modified Atmosphere Packaging. Sonklanakarin Journal of Science and Technology **2011**, *33*(2), 171–178.
20. Okpala, C.O.; Choo, W.S.; Dykes, G.A. Quality and Shelf Life Assessment of Pacific White Shrimp (*Litopenaeus Vannamei*) Freshly Harvested and Stored on Ice. LWT **2014**, *55*, 110–116.
21. Huidobro, A.; López-Caballero, M.; Mendes, R. Onboard Processing of Deepwater Pink Shrimp (Parapenaeus Longirostris) with Liquid Ice: Effect on Quality. European Food Research and Technology **2002**, *214*(6), 469–475.
22. Harper, A.M.; Duewer, D.L.; Kowalski, B.R.; Fashing, J.L. ARTHUR and Experimental Data Analysis. In *Chemometrics: Theory and Applications, ACS Symposium Series 52*; Kowalski, B.R.; Ed.; American Chemical Society Publisher: New York, NY, USA, 1977.
23. Quinlan, R. Discovering Rules From Large Collections of Examples: A Case Study. In *Expert Systems in the Microelectronic Age*; Michie, D.; Ed.; Edinburgh University Press: Edinburgh, Scotland, 1979; 168–201.
24. Breiman, L.; Friedman, J.H.; Olshen, R.A. Stone, C.J. *Classification and Regression Trees*; Wadsworth: Belmont, CA, 1983.
25. Heidarbeigi, K.; Mohtasebi, S.; Foroughirad, A.; Ghasemi-Varnamkhasti, M.; Rafiee, S.; Rezaei, K. Detection of Adulteration in Saffron Samples Using Electronic Nos. International Journal of Food Properties **2015**, *18*, 1391–1401.
26. Dowlati, M.; Mohtasebi, S.S.; Omid, M.; Razavi, S.H.; Jamzad, M.; de la Guardia, M. Freshness Assessment of Gilthead Sea Bream (*Sparus Aurata*) by Machine Vision Based on Gill and Eye Color Changes. Journal of Food Engineering **2013**, *119*(2), 277–287.